



## Influenza virus-like particles coated onto microneedles can elicit stimulatory effects on Langerhans cells in human skin

Marc Pearton<sup>a</sup>, Sang-Moo Kang<sup>b</sup>, Jae-Min Song<sup>b</sup>, Yeu-Chun Kim<sup>d</sup>, Fu-Shi Quan<sup>b</sup>, Alexander Anstey<sup>c</sup>, Matthew Ivory<sup>a</sup>, Mark R. Prausnitz<sup>d</sup>, Richard W. Compans<sup>b</sup>, James C. Birchall<sup>a,\*</sup>

<sup>a</sup> Welsh School of Pharmacy, Cardiff University, Cardiff, CF10 3NB, UK

<sup>b</sup> Department of Microbiology and Immunology, Emory University School of Medicine, Atlanta, GA 30332, USA

<sup>c</sup> Aneurin Bevan Health Board Royal Gwent Hospital, Cardiff Road, Newport, NP20 2UB, UK

<sup>d</sup> School of Chemical and Biomolecular Engineering, Georgia Institute of Technology, Atlanta, GA 30332, USA

### ARTICLE INFO

#### Article history:

Received 11 February 2010

Received in revised form 17 May 2010

Accepted 24 May 2010

Available online 8 June 2010

#### Keywords:

Influenza virus-like particle

Microneedles

Langerhans cell

### ABSTRACT

Virus-like particles (VLPs) have a number of features that make them attractive influenza vaccine candidates. Microneedle (MN) devices are being developed for the convenient and pain-free delivery of vaccines across the skin barrier layer. Whilst MN-based vaccines have demonstrated proof-of-concept in mice, it is vital to understand how MN targeting of VLPs to the skin epidermis affects activation and migration of Langerhans cells (LCs) in the real human skin environment. MNs coated with vaccine reproducibly penetrated freshly excised human skin, depositing 80% of the coating within 60 s of insertion. Human skin experiments showed that H1 (A/PR/8/34) and H5 (A/Viet Nam/1203/04) VLPs, delivered via MN, stimulated LCs resulting in changes in cell morphology and a reduction in cell number in epidermal sheets. LC response was significantly more pronounced in skin treated with H1 VLPs, compared with H5 VLPs. Our data provides strong evidence that MN-facilitated delivery of influenza VLP vaccines initiates a stimulatory response in LCs in human skin. The results support and validate animal data, suggesting that dendritic cells (DCs) targeted through deposition of the vaccine in skin generate immune response. The study also demonstrates the value of using human skin alongside animal studies for preclinical testing of intra-dermal (ID) vaccines.

© 2010 Elsevier Ltd. All rights reserved.

### 1. Introduction

Estimates indicate that in the United States alone there are 226,000 hospitalizations and 20–40,000 annual mortalities directly caused by seasonally circulating influenza viruses [1–3]. Sporadically, new forms of influenza virus appear to which the population at large has no previous exposure and as a corollary very limited protective immunity [4,5]. March 2009 saw the appearance of a new influenza A H1N1 strain. The rapid and extensive spread of the 2009 H1N1 virus resulted in the World Health Organization declaring phase 6 pandemic status on 11th June 2009 [6]. Previous influenza pandemics have been devastating, an estimated 50 million people died during the three influenza pandemics of the last century. Whilst the 2009 H1N1 strain displays higher infectivity compared to other influenza strains, fortunately the virus is not severely pathogenic and is responsive to anti-viral therapy [6]. However, as influenza virus strains differ greatly in their

pathogenicity, for example mortality rates associated with zoonotically acquired H5N1 avian influenza are extremely high [7], the potential impact of influenza pandemics should not be underestimated.

Vaccination offers the most economic and effective practical means of reducing morbidity and mortality associated with seasonal and pandemic influenza. However, current vaccination regimen can be limited by inadequate means to rapidly vaccinate the population against emergent threats. In the case of influenza this can be due to the time-consuming egg-based process used to produce vaccine [8]. As a result, new vaccine production methods, for example cell culture production [8–10] and plant bioreactors [11] and novel vaccines, including DNA vaccines [12,13] and VLPs [14], are being developed. VLPs have a number of advantages that make them attractive vaccine candidates. Having no viral genome VLPs are incapable of replication and therefore have a good safety profile. They are rapid to manufacture with a production time scale of weeks compared to months in the case of egg-based production. VLPs are also highly immunogenic, presenting antigen in a native form that requires no chemical inactivation [14].

Injectable influenza vaccines require cold storage and intramuscular (IM) injection by medically trained personnel, creating considerable logistical problems in distribution, storage and

\* Corresponding author at: Welsh School of Pharmacy, Redwood Building, King Edward VII Avenue, Cardiff, CF10 3NB, UK. Tel.: +44 2920875815; fax: +44 2920874149.

E-mail address: [birchalljc@cf.ac.uk](mailto:birchalljc@cf.ac.uk) (J.C. Birchall).

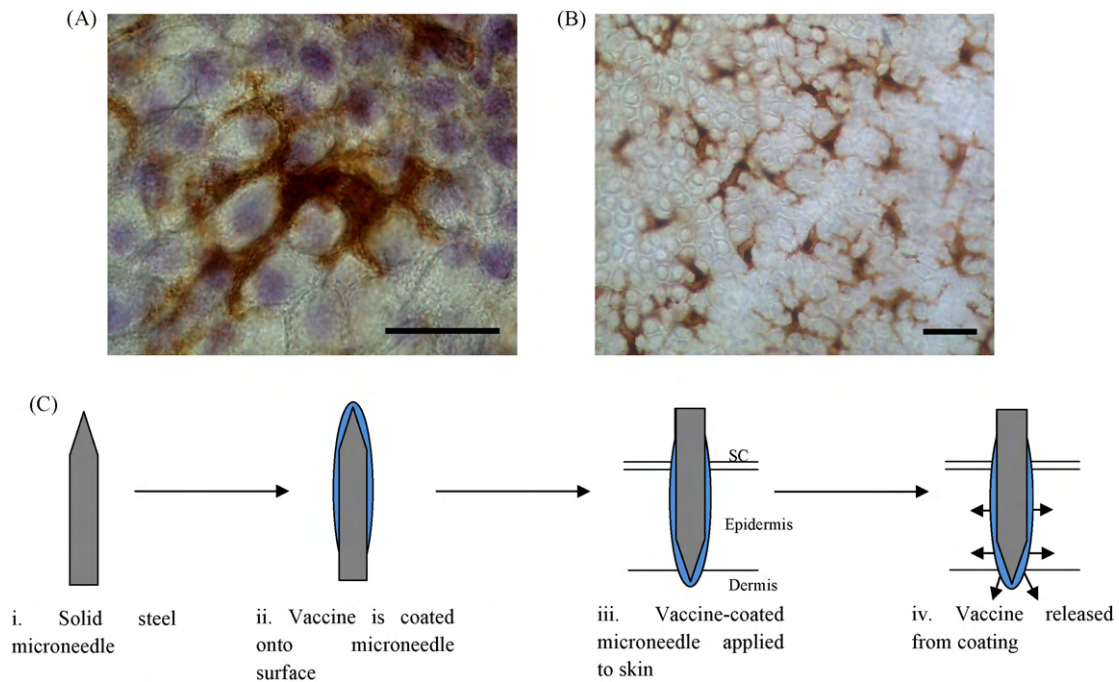


**Fig. 1.** Microneedle targeted delivery of vaccines to Langerhans cells in the epidermis. (A) An *en face* image of a single LC in epidermal sheet prepared from human skin showing distinctive dendritic cell morphology (bar = 10  $\mu\text{m}$ ). (B) At lower magnification the extensive network typical of LCs is apparent (bar = 10  $\mu\text{m}$ ). (C) Schematic showing the principle steps involved in delivering vaccines via coated MNs.

administration. MNs are being developed as a minimally invasive method for delivering therapeutics, including vaccines, across the skin barrier layer, the stratum corneum (SC) [15,16]. MNs are designed to transiently puncture the SC barrier allowing the delivery of material to underlying skin compartments exerting either a local or, following diffusion to the cutaneous circulation, systemic effect [17]. In the case of vaccination, MNs will facilitate intradermal or intra-epidermal targeting of the vaccine and thereby offers the potential to target the resident immune-responsive DCs (Fig. 1) to provide a more proficient immune response, potentially at lower dose when compared with IM delivery [18]. The potential advantages of MN-based immunization include the possibility of self-administration, opportunity for dose sparing, enhanced patient compliance and acquiescence with immunization schedules, reduced risk of needle stick injury and transmittance of infection, and ease of disposal. Furthermore, MN patches could rapidly be disseminated through pharmacies, public offices or even the postal system to enable rapid mass distribution in pandemic situations.

Recent studies have indicated that the delivery of vaccines by coated MNs provides immunological responses at least equal to, if not superior to, IM injection, based on: serum IgG antibody titres [19,20], viral titres in the lung [20–24], induction of neutralizing antibodies [20–24], cytokine response [20,24] and protection against viral challenge [19,24].

Whilst MN-based vaccines have therefore demonstrated proof-of-concept through the induction of a robust immune response and protection in mice, it is critically important to further explore how these data can be translated to human subjects. Given the acknowledged differences in the architecture and immune system of animal models [25], and the fact that MN technology aims to target specific layers and cell populations in human skin, it would be valuable to predict how MN targeting of vaccine to the skin epidermis affects immune activation in the real human skin environment. This study aims to exploit an established *ex vivo* human skin organ culture system [12,26,27] to test the performance of solid metal MNs in 'live' human skin and investigate the biological response to MNs

coated with influenza VLP candidate vaccines. The results complement studies using animal models, by testing the hypothesis that VLP vaccination in human skin with microneedles causes activation and migration of LCs and that the degree of LC activation and migration correlates with vaccine immunogenicity.

## 2. Materials and methods

### 2.1. MN fabrication and characterization

Arrays of solid metal MNs were fabricated by cutting needle structures from stainless steel sheets (McMaster-Carr, Atlanta, GA) using an infrared laser (Resonetics Maestro, Nashua, NH) and electropolishing as described previously [28]. MNs were imaged using both light microscopy (Olympus BX50 microscope, Olympus, Middlesex, UK) and scanning electron microscopy (SEM; Philips XL-20 SEM, Eindhoven, Netherlands).

### 2.2. Puncture of human skin by MN

All human skin samples were obtained from female patients undergoing mastectomy or breast reduction surgery under informed patient consent and local ethical committee approval. Excised skin was transported from surgery to the laboratory at 4 °C in 99% Dulbecco's modified Eagle medium (DMEM) and 1% penicillin/streptomycin (each at 100 IU mL<sup>-1</sup>). Excised human skin was prepared for treatment by removal of subcutaneous fat tissue by blunt dissection before being pinned, dermis side down, onto a cork dissection board. Following application of coated MNs, the treated regions of skin were excised, forming samples approximately 1 cm × 0.5 cm. These samples were cultured in a 6-well plate (4 samples per well) at the air liquid interface in a Trowel-type organ culture set-up. The culture media was composed of (DMEM) supplemented with 100 IU mL<sup>-1</sup> penicillin and 100 mg mL<sup>-1</sup> streptomycin. Organ culture was performed at 37 °C and 5% CO<sub>2</sub> [12,26,27].

### 2.3. Visualization of placebo MN puncturing human skin using SEM

MN were inserted into human skin and left *in situ*. The treated region of skin was carefully excised, rinsed in PBS, fixed in 2% (v/v) glutaraldehyde for 2 h at 4 °C and dehydrated in an ethanol gradient. Complete dehydration was achieved with a CPD030 critical point dryer (Bal-Tec, Balzers, Liechtenstein). Samples were mounted onto metal SEM stubs with double-sided carbon tape and sputter coated with gold (EM Scope, Kent, UK). Observations were made using a Philips XL-200 scanning electron microscope.

### 2.4. Evaluation of skin puncture by methylene blue staining and trans-epidermal water loss (TEWL)

MNs were applied to the surface of human skin for 10 s before removal; 20  $\mu$ L of 2% methylene blue solution was applied to the treated region followed by incubation at room temperature for 10 min. Excess methylene blue solution was then removed from the skin surface. Treated samples were briefly rinsed in PBS, fixed in 2% (v/v) glutaraldehyde for 2 h at 4 °C, and further rinsed in PBS before observation by light microscopy (Stemi 2000-C Stereomicroscope, Zeiss, Weyn Garden City, UK; Scott 1500 fibre optic external light source, Scott UK Ltd., Stafford, UK; Olympus DP-10 digital camera, Olympus Optical, London, UK). Water loss measurements of intact, untreated and MN-treated regions of *ex vivo* human skin was made using a hand-held TEWL probe connected to a Dermalab skin analysis system (Cortex Technology, Hadsund, Denmark).

### 2.5. Histological examination of MN-treated human skin

MN-treated skin samples were rinsed in PBS before fixation in formalin for 24 h. Samples were dehydrated in an ethanol gradient and cleared in chloroform prior to incubation in two changes of molten paraffin (56 °C) before embedding in fresh paraffin. Histological sections of 4  $\mu$ m were generated (Leica 2125 RT microtome, Milton Keynes, UK) and captured onto Superfrost® Plus slides (Fisher Scientific, Loughborough, UK) dried on a hot-plate, rehydrated and counter stained with hematoxylin. The depth of penetration achieved by MN application was determined in histological sections using ImageJ software (available at <http://rsb.info.nih.gov/ij/>; developed by Wayne Rasband, National Institutes of Health, Bethesda, MD, USA).

### 2.6. MN coating

Model and investigational materials were coated onto the surface of MNs using a micron-scale, dip-coating process, described in detail elsewhere [23,28,29].

#### 2.6.1. MN coating formulation

Placebo coating solutions were composed of 1% (w/v) carboxymethylcellulose sodium salt (CMC, Sigma–Aldrich Chemical Company, Poole, UK), 0.5% (w/v) Lutrol F-68 NF (BASF, Ludwigshafen, Germany) and 15% (w/v) trehalose as vaccine stabilizer (Sigma–Aldrich Chemical Company, Poole, UK) prepared in double distilled water ( $_{\text{dd}}\text{H}_2\text{O}$ ).

#### 2.6.2. Fluorescent nanospheres coating formulation

Coating solution prepared at double the concentration described in Section 2.6.1 was added to an equal volume of a suspension of fluorescent yellow/green or red polystyrene nanospheres (Sigma–Aldrich Chemical Company, Poole, UK; 10  $\mu$ L nanospheres concentrate was diluted in 990  $\mu$ L  $_{\text{dd}}\text{H}_2\text{O}$ ). Coated MNs were dried overnight, protected from light.

### 2.6.3. Methylene blue coating formulation

Coating solution prepared at double the concentration, as described above, was added to an equal volume of 4% (w/v) methylene blue (Fisher Scientific, Loughborough, UK) prepared in  $_{\text{dd}}\text{H}_2\text{O}$ .

### 2.6.4. H1 and H5 virus-like particle (VLP) coating formulations

Influenza H1 and H5 VLPs containing hemagglutinin (HA) and matrix (M1) proteins derived from A/PR/8/34 (H1N1) or A/Viet Nam/1203/2004 (H5N1) were prepared as described [14,22]. To produce influenza VLP vaccine, Sf9 insect cells were co-infected with recombinant baculoviruses (BVs) expressing HA and M1. Influenza VLPs in the culture supernatants were purified by using discontinuous sucrose gradient layers, and characterized by Western blot and hemagglutination activity analysis [22]. The contents of HA in H1 VLPs were determined by hemagglutination activity in comparison with that of inactivated virus at the same concentration (1 mg mL<sup>-1</sup>) and confirmed by quantitative Western blot of VLPs and inactivated virus (1–5  $\mu$ g protein per well) [22]. The HA content in H1 VLPs was estimated based on the observation that influenza virus HA makes up approximately 29% of the total proteins of purified virus [31]. The HA content in H5 VLPs was similarly determined by hemagglutination assay which gave approximately a 3:1 ratio of H5 inactivated virus to VLPs and also confirmed by Western blot analysis using the purified recombinant H5 HA protein as a standard (Song et al., unpublished data). The content of HA was approximately 10% of total proteins of influenza VLPs, which is similar to that of a previous report [22]. Double concentration coating solution, as described in Section 2.6.1, was added to an equal volume of H1 and H5 VLPs (100  $\mu$ g mL<sup>-1</sup>) prepared in  $_{\text{dd}}\text{H}_2\text{O}$ . Coated MNs with VLP vaccines were either used for *ex vivo* human skin organ culture studies or directly to immunize mice on the skin for testing vaccine efficacy.

### 2.7. Characterization of coated MNs

MNs coated with fluorescent nanospheres were mounted onto SEM stubs with double-sided carbon tape before sputter coating with gold. Visual observations were made using a Philips XL-200 scanning electron microscope. The same MNs were visualized using an Olympus BX50 fluorescent microscope with digital image capture.

### 2.8. Dissolution of coated formulation in *ex vivo* human skin

#### 2.8.1. Measurement of fluorescence

Fluorescently coated MNs were inserted into excised human skin and left *in situ* for 10, 30 or 60 s ( $n=4$  for each group) before removal. The MNs were observed using an Olympus BX50 fluorescent microscope with a digital camera. The area of remaining fluorescence, with respect to the total area of the MN, was determined using ImageJ software.

#### 2.8.2. Visualization using methylene blue

MNs coated with methylene blue dye remained in the skin for 5 min before removal ( $n=4$ ). Treated regions were excised, fixed in 2% (v/v) glutaraldehyde for 2 h at 4 °C, rinsed in PBS prior to observation by light microscopy, images were digitally recorded.

### 2.9. Changes in LC distribution in human skin following treatment with H1 and H5 VLPs coated onto MNs

The response of LCs behavior to H1 and H5 VLPs was assessed in epidermal sheets and histological sections following immunohistochemistry (IHC), where the primary antibody was a mouse monoclonal against CD207 (Langerin).

### 2.9.1. Generation of epidermal sheets and IHC

Following insertion of H1 and H5 VLP-coated MNs for 5 min, skin samples were incubated in 3.8% w/v ammonium thiocyanate (Sigma–Aldrich Chemical Company, Poole, UK) in PBS for 20–40 min. The epidermis was peeled away from the dermis with forceps under a dissection microscope (Leica 200M 2000, Milton Keynes, UK). Epidermal sheets were fixed in pre-cooled acetone at  $-20^{\circ}\text{C}$  for 20 min followed by rinsing in PBS. The sheets were transferred into 1.5 mL centrifuge tubes and incubated in 0.03% (v/v)  $\text{H}_2\text{O}_2$  for 5 min at room temperature. Peroxide solution was removed by pipetting before 1 mL of PBS/Tween (0.01 M PBS; 0.05% Tween-20 adjusted to pH 7.4) was added for 3 min and removed; this was repeated a total of 3 times. The primary CD207 (Langerin) mouse monoclonal antibody (12D6, Abcam, Cambridge, UK) was diluted 1/100 and incubated at room temperature for 1 h. Sheets were rinsed in three changes of 1 mL PBS/Tween, each for 3 min. Detection of primary antibody was achieved with EnVision+ system-HRP (DAB) kit (Dako UK Ltd., Cambridgeshire, UK) according to the manufacturer's specifications. Sheets were spread out on slides and visualized by light microscopy with representative images captured digitally (Olympus, Watford, UK). Image analysis was performed with ImageJ software. To determine cell number, IHC-stained epidermal sheets were viewed at  $20\times$  magnification, corresponding to a field of view of  $360$  by  $450\ \mu\text{m}$ , and random images were captured ( $n=50$ ) for each treatment and time point, from which the number of cells were counted and averaged.

### 2.9.2. Generation of histological sections and IHC

Following insertion of H1 and H5 VLP-coated MNs for 5 min, skin sections were obtained as previously described. Selected slides were rehydrated through an ethanol gradient and subjected to heat-mediated antigen retrieval in Tris–EDTA buffer (10 mM Tris base; 1 mM EDTA; 0.05% (v/v) Tween 20, in  $1\ \text{L}_{\text{dd}}\text{H}_2\text{O}$  adjusted to pH 9.0) at approximately  $95^{\circ}\text{C}$  for 40 min; following which the slides were maintained in antigen retrieval buffer but removed from heat and allowed to cool for approximately 20 min at room temperature. Slides were washed in two changes of PBS–Tween before incubation in 0.03%  $\text{H}_2\text{O}_2$  for 5 min at room temperature. The primary CD207 (Langerin) mouse monoclonal antibody (12D6, Abcam, Cambridge, UK) was diluted 1/100 and incubated at  $4^{\circ}\text{C}$  overnight in a humidified chamber. Primary antibody detection was achieved with by EnVision+ system-HRP (DAB) kit according to the manufacturer's specifications and visualized by light microscopy with images captured for analysis (Olympus). The percentage area occupied by LCs in histological sections was determined relative to the total epidermal area using ImageJ software.

### 2.10. Immunization of mice with VLP-coated MNs

BALB/c mice (females, 6–8 weeks of age) purchased from Harlan Laboratories were housed in microisolator units under the approved Emory University IACUC protocol for laboratory animals. Mice ( $n=6$ ) were immunized with a MN array coated with VLP vaccine for delivery to the skin. The placebo control group was similarly treated using a MN with coating solution but without VLP vaccine. For MN vaccination, mice were anesthetized with ketamine (110 mg/kg, Abbott Laboratories, Abbott Park, IL, USA) mixed with xylazine (11 mg/kg, Phoenix Scientific, Saint Joseph, MO, USA). Hair on the dorsal surface of mice was removed by depilatory cream, and an array of VLP vaccine-coated MNs was inserted into the skin for 10 min for release of the vaccine antigen from the coated MNs. The levels of serum antibodies were determined using inactivated virus as an ELISA coating antigen by following a procedure previously described [14,22].

### 2.11. Statistical analysis

Statistical significance in human explant studies was determined by one-way analysis of variance (ANOVA) followed by Tukey's post hoc analysis. A two-tailed paired Student's *t*-test was performed when comparing two groups of animals.

## 3. Results

### 3.1. MN fabrication and characterization

Arrays of stainless steel MNs were fabricated by laser etching stainless steel sheets. Devices consisted of rows containing five MNs, equally spaced by 1.5 mm. Individual MN height was determined to be  $700\ \mu\text{m}$  with a width, at the base, of  $50\ \mu\text{m}$  tapering into a sharp point [28].

### 3.2. Puncturing of human skin by MNs

MN devices applied to freshly excised human skin with minimal application force effortlessly punctured through the SC (Fig. 2A). Upon removal, no significant deformation or other damage to the MNs was observed (Fig. 2B). MN treatment resulted in the formation of discrete puncture sites through the SC as visualized by post-staining treated skin samples with 2% (w/v) methylene blue staining (Fig. 2B). Transverse sectioning revealed that these punctures extended through the epidermis into the upper region of the dermis to a depth of typically between 200 and  $500\ \mu\text{m}$  (Fig. 2C). The discrepancy between MN height and depth of penetration is a result of the innate skin elasticity and the resultant deformation caused to the skin during application and the difficulty in pinpointing maximum depth of penetration using histological sections. A significant ( $p < 0.05$ ) increase in trans-epidermal water loss (TEWL) was recorded in MN-treated skin compared to untreated skin (Fig. 2D). These studies demonstrate that these MNs easily and reproducibly compromised the SC barrier of viable human skin.

### 3.3. MN coating and dissolution following application to ex vivo human skin

MNs were coated by a gentle, room temperature process involving a water-based coating solution containing excipients with established safety and FDA approval for use in other parenteral delivery systems [28]. The dip-coating apparatus and procedures allowed for deposition of a uniform coat over the entire surface of each MN (Fig. 3A and B). Although the coating covered the whole MN, including the tip, there appeared to be little reduction in sharpness (Fig. 3A and B). Consequently, there was no need to alter the force required to penetrate human skin with a coated MN compared to an uncoated MN.

When MNs coated with fluorescent nanospheres were inserted into *ex vivo* human skin, the coating formulation was rapidly dissolved and released the coated payload within skin (Fig. 3C). Although the coating formulation was coated over the entire surface of each MN, the coating did not appear to deposit uniformly following MN insertion into skin. Dissolution of the formulation was more rapid at the tip region of the MN, taking slightly longer as the MN descended toward the base (Fig. 3C inserts). This was probably due to incomplete insertion of the microneedle to its full length in the skin and thinner coating near the MN tip due to effects of curvature on surface tension during the dip-coating process. Overall, more than 80% of the coating was deposited in skin within 60 s of insertion.

Deposition of coated payload from the MNs was confirmed using MNs coated with methylene blue dye. After 5 min application of

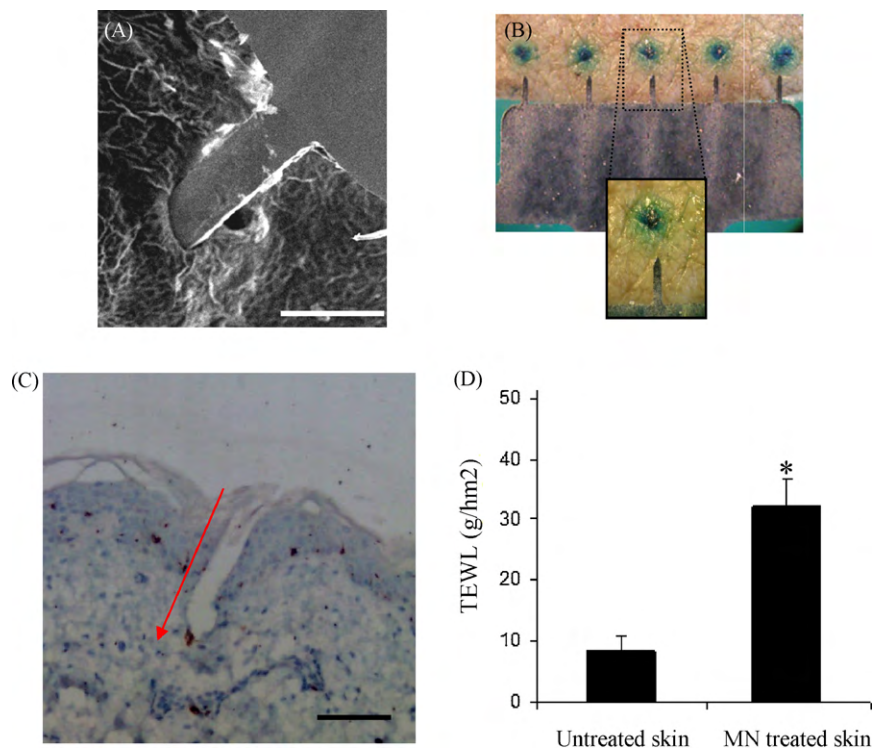


**Fig. 2.** Microneedles effectively penetrate human skin. (A) SEM study of a MN penetrating human SC *in situ* (bar = 300  $\mu\text{m}$ ). Human skin treated with MNs resulted in the formation of discrete channels through the SC, as revealed by methylene blue staining (B) and histological sections (5  $\mu\text{m}$ ) that reveal MN penetration through the SC and epidermis and into the upper reaches of the dermis; red arrow indicates direction of MN application (C; bar = 150  $\mu\text{m}$ ). MN penetration was associated with an increase in trans-epidermal water loss (D); data presented as mean  $\pm$  SD ( $n = 10$ ), two replicates. Significance was determined relevant to blank skin ( $*p \leq 0.05$ ). (For interpretation of the references to colour in this figure legend, the reader is referred to the web version of the article.)

the device, and surface swabbing with 70% ethanol to remove surface contamination, discrete blue regions of staining caused by dye release from the microneedle surface were observed corresponding to regions punctured by individual MNs (Fig. 3D).

#### 3.4. Changes in LC numbers following treatment with VLP-coated MNs

Excised human skin explants were used to monitor changes in the population of resident LC in response to MN-assisted delivery of VLP vaccines. We were interested to study LC migration from the epidermis because it is an essential prerequisite for antigen presentation in the lymph nodes. The excision and culture of human skin resulted in a depletion in LC number over time as a result of physical and chemical damage to the tissue and subsequent release of migratory signals [12,30,32]. It was also observed that this phenomenon occurred during control studies of untreated skin and skin treated with placebo MNs (Fig. 4A and B), where the depletion of LCs occurs at a statistically identical rate ( $p > 0.05$ ) (Fig. 4A). This observed depletion of LC numbers in untreated and placebo MN-treated skin samples can be regarded as the baseline against which subsequent treatments can be measured.

Against this background, noticeable effects on LC numbers and morphology were observed following cutaneous delivery of H1 and H5 VLPs via MNs. Epidermal sheets prepared 24 h after treatment showed that LC numbers in skin samples treated with MN coatings of H5 VLPs were significantly reduced ( $p < 0.05$ ) compared to untreated skin samples (Fig. 4A). The reduction in LCs numbers was also apparent 48 h after treatment. Additionally, the microscopic appearance of epidermal sheets stained for LCs differed significantly for skin treated with MNs coated with H5 VLPs compared with untreated cultured skin at each time point (Fig. 4B). When MNs coated with H1 VLPs were administered to skin, the reduction

in LC numbers in the plane of the epidermal sheet was statistically ( $p < 0.05$ ) more pronounced than for skin treated with H5 VLPs, indicating a difference in the stimulatory capability of the two VLP candidate vaccines. The more defined changes in the LC population following delivery of the H1 VLPs via MNs are further supported in Fig. 4B.

#### 3.5. Changes in LC distribution and area in histological skin sections

The total area occupied by LCs, i.e., the LC area as a percentage of total cell area, in transverse sections of untreated skin remained relatively consistent over the culture period (0–48 h; Fig. 5). Untreated sections revealed LCs to be typically rounded and well spaced out throughout the epidermis, with no noticeable overlapping of cells (Fig. 5A). In contrast, sections of skin following H1 and H5 VLP treatment via MNs showed a significant ( $p < 0.001$ ) change in the area occupied by LCs (Fig. 5A). The change in area following treatment with VLPs was accompanied by a clear change in LC morphology and distribution pattern, which are indicative of activated and subsequently migratory LCs [30].

Fig. 5B–D shows representative images of untreated skin sections and H5 and H1 VLP MN-treated sections respectively. Whilst skin sections following MN application provide no visual evidence of skin puncture, presumably as aberrations in the SC would have largely resealed during the 24-h culture period, our procedures ensure that the sections shown in Fig. 5 represent areas in proximity to the MN treatment. The LCs in sections taken from VLP-treated skin samples appear to be more dispersed throughout the epidermis and less uniform in distance from one another (Fig. 5C and D). In the case of the H1 VLP-treated samples, the LCs appear more elongated and longitudinal to the basement membrane (Fig. 5D). At 48 h, the area occupied by LC in epidermal sections was reduced, approaching pre-culture levels (Fig. 5A).

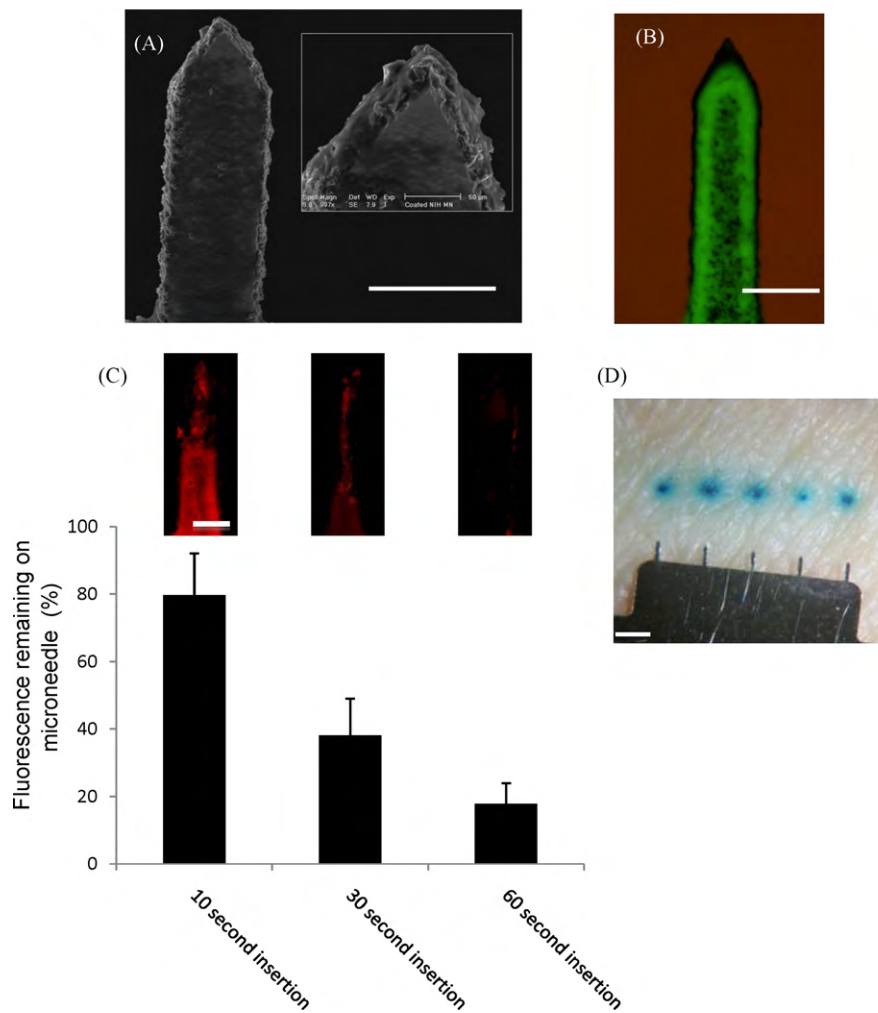


**Fig. 3.** Coating microneedles and dissolution of coating in excised human skin. (A) SEM images of a single MN coated with fluorescent nanospheres (bar = 200 μm). (B) Bright field plus fluorescence microscopy of a single MN coated with fluorescent nanospheres (bar = 200 μm). (C) Amount of fluorescently coated material remaining on MN surface following insertion into human skin; data presented as mean percentage fluorescence remaining ± SD ( $n = 4$ ), two replicates. Representative images of entire single needles from corresponding time points are shown as inserts (bar = 50 μm). (D) MNs coated with methylene blue demonstrate dissolution and deposition of the coated material within the skin (bar = 1 mm).

### 3.6. Comparison of immunogenicity of H1 and H5 MN vaccines delivered to mouse model

As a means to confirm the functionality of the VLP vaccines and to enable comparison with observations in viable human skin, the immunogenicity of MN vaccine delivery of the same influenza H1 and H5 VLPs was tested in a mouse model. Virus-specific antibody responses were determined at week 4 after a single MN vaccination with 0.4 μg H1 or H5 VLPs in the skin (Fig. 6). The levels of antibodies specific to A/PR8 (H1N1) were statistically ( $p < 0.01$ ) higher in the H1 VLP group compared to those specific to A/Viet Nam/1203/04 (H5N1) in the H5 VLP group (i.e., in both cases, antibody titres were determined for the influenza strain homologous to the vaccine given). Although determining the antibody levels is not an absolute comparison due to several factors, including different antigens, these data indicate that the H1 VLPs were more immunogenic than H5 VLPs used in this study.

## 4. Discussion

The aims of the current study were to test the hypothesis that VLP vaccination in human skin with MNs causes migration of LC and that the degree of LC migration correlates with vaccine immuno-

genicity. The effects of VLP vaccine on LCs was assessed in this study principally because they are the most accessible and easily monitored DC subtype to be investigated in the correct biological context. Whilst the role of DDCs is not considered here their role in generating immunity *in vivo* should not be ignored.

As discussed below, we believe the results of this study support this hypothesis. VLP vaccination using MN caused increased LC activation and migration indicated by changes in LC morphology and numbers in *ex vivo* skin. H1 VLPs caused greater stimulation of LCs resulting in a significant increase in migratory cells than H5 VLPs. This observation is interesting because *in vivo* immunogenicity results obtained in mice, showed H1 VLPs generated stronger virus-specific antibody responses in contrast to H5 VLPs. This observation suggests that stimulated, migratory LC may play a significant role in generation of antibody responses following VLP vaccination using MNs.

The results also provide further proof-of-concept of this MN vaccination approach, as they are the first to show that novel vaccine candidates delivered as a surface coating on microfabricated MNs have a stimulatory effect on live, functional human DCs in the biologically relevant environment of viable human skin. Consequently, the present study also demonstrates the utility of using this human skin model alongside animal studies for relevant preclinical testing of ID vaccines.

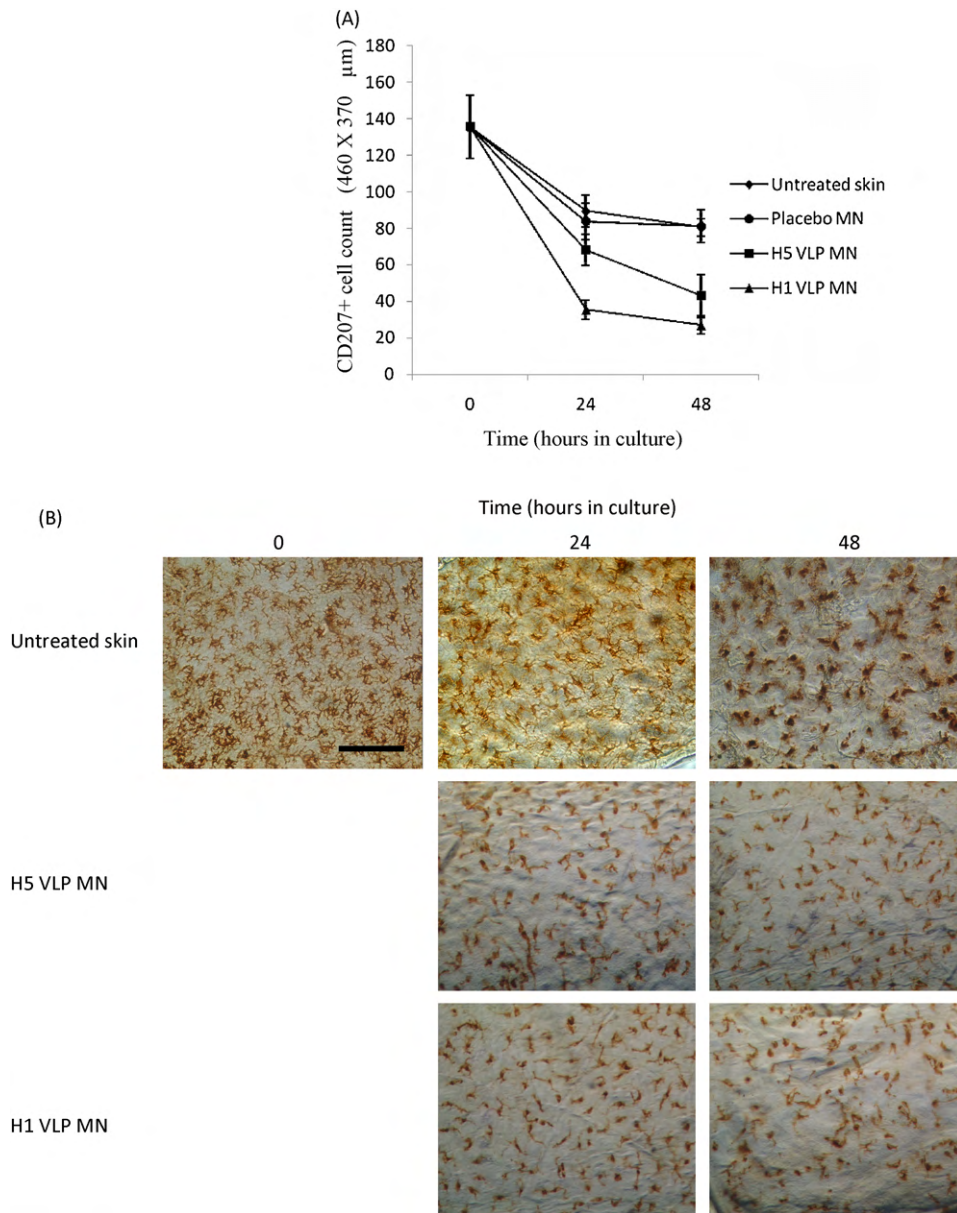


**Fig. 4.** Reduction in LC numbers in epidermal sheets. (A) Blank skin (◆); blank coated MNs containing no VLP (●); H1 VLPs (▲) and H5 VLPs (■) delivered from coated MNs; data presented as mean  $\pm$  SD ( $n=4$ ), one replicate. (B) Representative images of LC from each time point and treatment (bar = 100  $\mu\text{m}$ ).

The MNs used in this study were micro-machined from stainless steel, which is a low-cost, well-tolerated and FDA-approved material. The material properties and structural morphology of the MNs permitted easy and consistent puncture of freshly excised human skin, through the epidermis into the upper reaches of the dermis, thereby targeting the resident antigen-presenting cells; principally the LCs of the epidermis and dermal DCs of the dermis. In addition to enhancing the penetrative capabilities of the MNs, this MN design is also well suited to dip coating [19,23,28,29]. Importantly, coatings remained attached to the MNs during application to viable human skin.

Following skin insertion MN coatings were able to dissolve; this being a relatively rapid process with approximately 80% of the payload delivered after 1 min and only negligible amounts remaining after 5 min. The dissolution experiments presented here are the first such studies performed in freshly excised human skin. These studies suggest that MN dissolution is a non-uniform process, i.e., the coating is released from the MN tip first followed by the remainder

of the needle shaft, presumably as a combined function of incomplete insertion of the MN, reduced coating thickness at the MN tip and increased hydration of the tip component in the deeper and more aqueous dermis compartment. The subsequent fate of the delivered material including the degree of cellular uptake is currently under investigation.

The focus of this study was to observe and monitor changes in LC behavior in viably maintained excised human skin exposed to influenza VLP vaccines. Two VLP vaccines were chosen for this study due to their current relevance to human health, i.e., swine (H1) and avian (H5) influenza. Freshly excised human skin was maintained viable in organ culture following the insertion of 5 MNs coated with either H1 or H5 VLP vaccines. Untreated skin was also cultured as control. Epidermal sheets were generated from cultured skin samples at 24 or 48 h and stained by immunohistochemistry (IHC) for CD207, a characteristic marker for LCs. LCs are peripheral DCs that, once stimulated, migrate from the site of antigen uptake to present the antigen to naïve T-cells in draining lymph nodes.

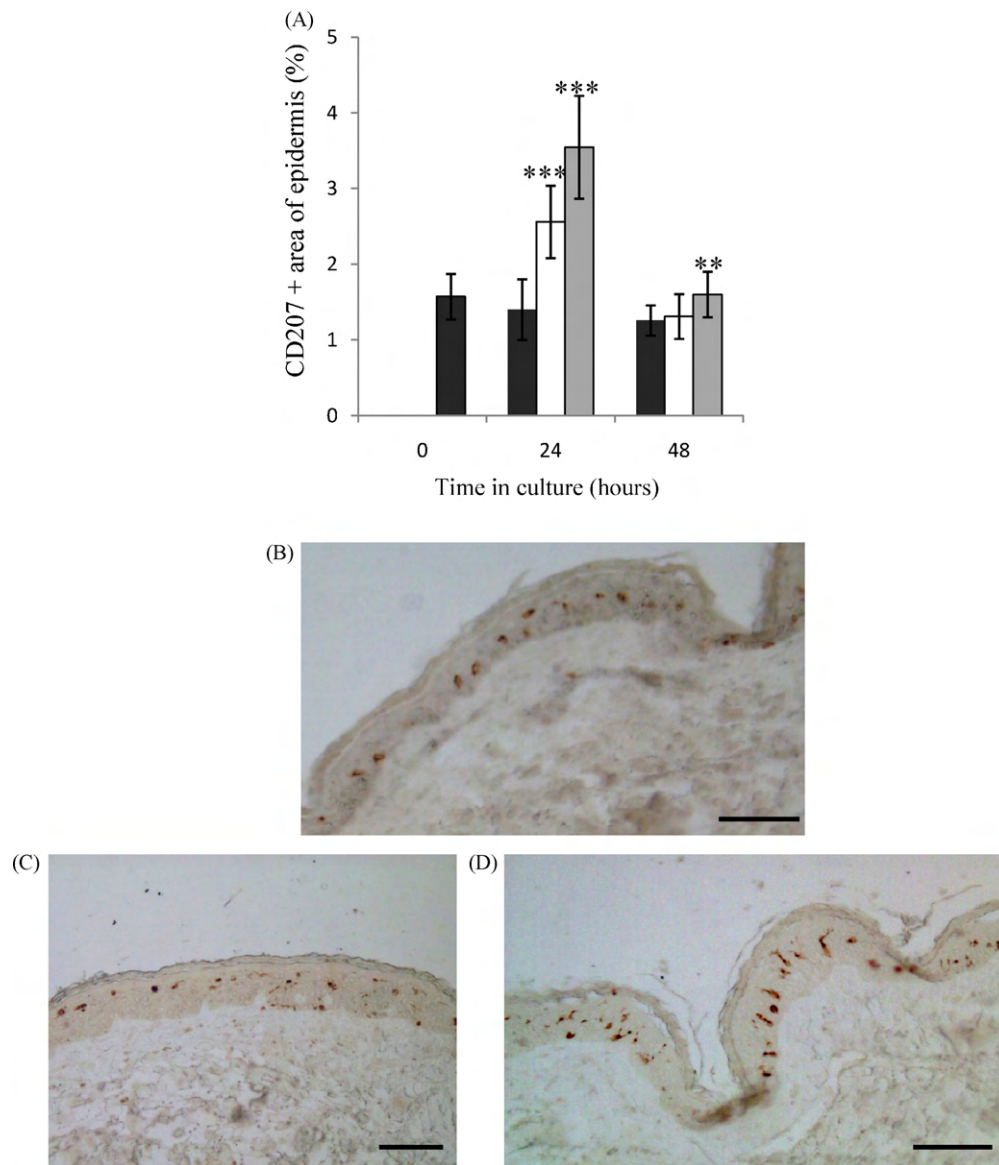


**Fig. 5.** Area and distribution of LC in histological sections. (A) The area of histological skin sections staining positive for CD207; blank skin (black bars), H5 VLP MN treated (white bars), H1 VLP MN treated (grey bars). Data presented as mean  $\pm$  SD ( $n=4$ ), one replicate. Significance was determined relative to blank skin at corresponding time point (\* $p \leq 0.05$ , \*\* $p \leq 0.01$ , \*\*\* $p \leq 0.001$ ). (B–D) The distribution of LC in histological skin sections: blank skin (B); skin treated with H5 and H1 VLPs delivered from coated MNs (C and D, respectively). All images taken from sections of cultured skin samples 24 h post-treatment (bar = 50  $\mu$ m in all cases).

The number of LCs in epidermal sheets depleted significantly more rapidly from samples treated with H1 and H5 VLPs delivered via MNs compared to untreated skin. A reduction in LC number in a given plane of the epidermis therefore provides an indication of LC migration in response to intra-epidermal vaccine delivery. Interestingly, LC response was significantly more pronounced in skin treated with the H1 VLPs compared with the H5 VLPs. This observation is important from two perspectives. Firstly, the data suggest that H1 VLP vaccines may be more stimulatory to antigen-presenting cells. Secondly, the fact that LCs resident within excised human skin are able to respond differently to two different vaccines, and not respond above baseline to a placebo MN insertion containing no vaccine, shows that the human skin model is discriminatory and may therefore inform selection of optimal vaccines based upon LCs response in the relevant local environment of human skin.

Previous clinical and animal studies demonstrated potential differences in immunogenicity among influenza vaccine antigens. In particular, the H5 vaccine antigens were demonstrated to induce

relatively weak immune responses, requiring high doses of vaccine compared to the seasonal influenza vaccine antigens [33–35]. Our current study provides evidence that H1 VLPs delivered via MNs induced higher levels of antibody responses in mice than H5 VLPs. In addition, we found that a higher dose of H5 VLP MN vaccines or prime-boost vaccination regimen might be needed to induce comparable protection against A/Viet Nam/1203/04 than the H1 A/PR8 MN vaccine (unpublished data). Also, H1 VLPs (A/PR8) could confer protective immunity at a lower dose than H5 VLPs (A/Viet Nam/1203/04) when intranasal immunization of mice was compared [14,22].

Comparing the human skin data with such studies is critical to ensure that any observations of local immune cell stimulation in the human skin model are not overplayed. Indeed, in the development of MNs, and other, vaccines it could be important to demonstrate both local targeting to appropriate cell types in the human setting and generation of systemic immune response in animal models to provide a complementary and meaningful data set to progress to clinical studies. Further, comparison of observations obtained from

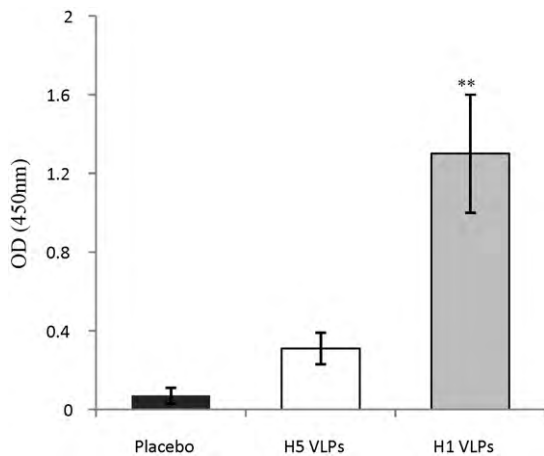


**Fig. 6.** Comparison of immunogenicity of H1 and H5 MN vaccines delivered to mice. Groups of mice ( $n=6$ ) were vaccinated in the skin using MNs coated with  $0.4 \mu\text{g}$  of H1 VLPs (A/PR8) or H5 VLPs (A/Viet Nam/1203/04). Placebo is the group that received MNs without vaccine. At week 4 after vaccination, serum samples were collected from individual mice and used to determine virus-specific antibody responses. Inactivated A/PR8 (H1N1) and reassortant A/Viet Nam/1203/04 (H5N1) viruses were used as a coating antigen for ELISA of H1 VLP and H5 VLP groups respectively. Values of optical density at 450 nm were shown with  $400\times$  diluted samples. Results represent data from at least two independent experiments and three independent serum antibody analyses.  $**p < 0.01$  compared with H5 VLP group.

animal and human models may provide mechanistic information to increase understanding and influence the optimal design of both MNs and vaccine modalities.

Direct *en face* observation of human epidermal sheets suggests that H5 and particularly H1 VLP-treated samples contained high proportions of LCs displaying a more rounded, and less dendritic, morphology, which were not as apparent in untreated skin samples from corresponding time points. It is proposed that these morphological changes observed in the VLP-treated samples are cells actively in the process of preparing and in the active process of migration. When comparable samples were examined in histological sections, at equivalent time points, there was a noticeable increase in LCs area at 24 h. Histological sections of skin treated with VLPs also showed that LCs were more dispersed throughout the epidermis 24 h after treatment. Furthermore, in the case of skin treatment with H1 VLPs via MNs, a number of LCs appeared vertically elongated with respect to the skin surface, suggesting active movement of cells from the central epidermis towards the basement membrane and beyond. These fascinating observations of changes in LC morphology, spatial arrangement and temporal distribution throughout the epidermis (and dermis) in response to ID vaccination are currently under more detailed investigation.

In summary, our data provide strong evidence that MN-facilitated delivery of influenza VLP vaccines can initiate a response in LC behavior in excised human skin epidermis. Simultaneous assessment of localized delivery and resulting functional response supports *in vivo* data from mice presented here and elsewhere [19,20,23,24,36] by showing that the observed effects in animals are indeed likely to be caused at least in part by immune activation generated by DCs targeted through deposition of the vaccine in skin. Further, as we show consistency between levels of systemic immune response and local effects on LCs for different antigens, this suggests a relationship, and possibly a causative relationship, between targeting and/or stimulation of LCs and improved immunogenicity. The human skin model can therefore potentially be used to help ascertain which delivery modalities and antigens are likely to produce greater immune response following cutaneous delivery.

## Acknowledgment

This work was funded by the National Institutes of Health Grant EB006369.

## References

- [1] Chen WH, Kozlovsky BF, Effros RB, Grubeck-Loebenstien B, Edelman R, Szein MB. Vaccination in the elderly: an immunological perspective. *Trends Immunol* 2009;30(7):351–9.
- [2] Nistal-Villán E, García-Sastre A. New prospects for the rational design of antivirals. *Nat Med* 2009;15(11):1253–4.
- [3] Fiore AE, Shay DK, Broder K, Iskander JK, Uyeki TM, Mootrey G, et al. Prevention and control of influenza: recommendations of the Advisory Committee on Immunization Practices (ACIP), 2008. *MMWR Recomm Rep* 2008;57:1–60.
- [4] Capua I, Alexander DJ. Ecology, epidemiology and human health implications of avian influenza viruses: why do we need to share genetic data? *Zoonoses Public Health* 2008;55(1):2–15.
- [5] Greenbaum JA, Kotturi MF, Kim Y, Oseroff C, Vaughan K, Salimi N, et al. Pre-existing immunity against swine-origin H1N1 influenza viruses in the general human population. *Proc Natl Acad Sci USA* 2009;106(48):20365–70.
- [6] Jones JH, Salathé M. Early assessment of anxiety and behavioural response to novel swine-origin influenza A(H1N1). *PLoS One* 2009;4(12):e8032.
- [7] Wan XF, Nguyen T, Davis CT, Smith CB, Zhao ZM, Carrel M, et al. Evolution of highly pathogenic H5N1 avian influenza viruses in Vietnam between 2001 and 2007. *PLoS One* 2008;3(10):e3462.
- [8] Genzel Y, Reichl U. Continuous cell lines as a production system for influenza vaccines. *Expert Rev Vaccines* 2009;8(12):1681–92.
- [9] Meghrou J, Mahmoud W, Jacob D, Chubet R, Cox M, Kamen AA. Development of a simple and high-yielding fed-batch process for the production of influenza vaccines. *Vaccine* 2009;28(2):309–16.
- [10] Keitel WA, Dekker CL, Mink C, Campbell JD, Edwards KM, Patel SM, et al. Safety and immunogenicity of inactivated, Vero cell culture-derived whole virus influenza A/H5N1 vaccine given alone or with aluminum hydroxide adjuvant in healthy adults. *Vaccine* 2009;27(47):6642–8.
- [11] Golovkin M, Spitsin S, Andrianov V, Smirnov Y, Xiao Y, Pogrebnyak N, et al. Smallpox subunit vaccine produced in *Planta* confers protection in mice. *Proc Natl Acad Sci USA* 2007;104(16):6864–9.
- [12] Ng KW, Pearton M, Coulman S, Anstey A, Gateley C, Morrissey A, et al. Development of an *ex vivo* human skin model for intradermal vaccination: tissue viability and Langerhans cell behavior. *Vaccine* 2009;27:5948–55.
- [13] Garmory H, Brown K, Titball R. DNA vaccination: improving expression of antigens. *Genet Vaccine Ther* 2003;1(1):2 [accessed on 07.01.10], available at: <http://www.gvt-journal.com/content/1/1/2>.
- [14] Kang SM, Yoo DG, Lipatov AS, Song JM, Davis CT, Quan FS, et al. Induction of long-term protective immune responses by influenza H5N1 virus-like particles. *PLoS One* 2009;4(3):e4667.
- [15] Prausnitz MR, Mikszta JA, Cormier M, Andrianov AK. Microneedle-based vaccines. *Curr Top Microbiol Immunol* 2009;333:369–93.
- [16] Coulman S, Allender C, Birchall J. Microneedles and other physical methods for overcoming the stratum corneum barrier for cutaneous gene therapy. *Crit Rev Ther Drug Carrier Syst* 2006;23(3):205–58.
- [17] Wang PM, Cornwell M, Hill J, Prausnitz MR. Precise microinjection into skin using hollow microneedles. *J Invest Dermatol* 2006;126(5):1080–7.
- [18] Leroux-Roels I, Vets E, Freese R, Seiberling M, Weber F, Salamand C, et al. Seasonal influenza vaccine delivered by intradermal microinjection: A randomised controlled safety and immunogenicity trial in adults. *Vaccine* 2008;26(51):6614–9.
- [19] Zhu Q, Zarnitsyn VG, Ye L, Wen Z, Gao Y, Pan L, et al. Immunization by vaccine-coated microneedle arrays protects against lethal influenza virus challenge. *Proc Natl Acad Sci USA* 2009;106(19):7968–73.
- [20] Koutsonanos DG, del Pilar, Martin M, Zarnitsyn VG, Sullivan SP, Compans RW, et al. Transdermal influenza immunization with vaccine-coated microneedle arrays. *PLoS One* 2009;4(3):e4773.
- [21] Quan FS, Kim YC, Yoo DG, Compans RW, Prausnitz MR, Kang SM. Stabilization of influenza vaccine enhances protection by microneedle delivery in the mouse skin. *PLoS One* 2009;4(9):e7152.
- [22] Quan FS, Yoo DG, Song JM, Clements JD, Compans RW, Kang SM. Kinetics of immune responses to influenza virus-like particles and dose-dependence of protection with a single vaccination. *J Virol* 2009;83(9):4489–97.
- [23] Kim YC, Quan FS, Compans RW, Kang SM, Prausnitz MR. Formulation and coating of microneedles with inactivated influenza virus to improve vaccine stability and immunogenicity. *J Control Release* 2010;142(2):187–95.
- [24] Kim YC, Quan FS, Yoo DG, Compans RW, Kang SM, Prausnitz MR. Improved influenza vaccination in the skin using vaccine coated microneedles. *Vaccine* 2009;27(49):6932–8.
- [25] Mestas J, Hughes CCW. Of mice and not men: differences between mouse and human immunology. *J Immunol* 2004;172:2731–8.
- [26] Pearton M, Allender C, Brain K, Anstey A, Gateley C, Wilke N, et al. Gene delivery to the epidermal cells of human skin explants using microfabricated microneedles and hydrogel formulations. *Pharm Res* 2008;25(2):407–16.
- [27] Birchall J, Coulman S, Pearton M, Allender C, Brain K, Anstey A, et al. Cutaneous DNA delivery and gene expression in *ex vivo* human skin explants via wet-etch micro-fabricated micro-needles. *J Drug Target* 2005;13(7):415–21.

- [28] Gill HS, Prausnitz MR. Coated microneedles for transdermal delivery. *J Control Release* 2007;117(2):227–37.
- [29] Gill HS, Prausnitz MR. Coating formulations for microneedles. *Pharm Res* 2007;24(7):1369–80.
- [30] Nishibu A, Ward BR, Boes M, Takashima A. Roles for IL-1 and TNFalpha in dynamic behavioral responses of Langerhans cells to topical hapten application. *J Dermatol Sci* 2007;45(1):23–30.
- [31] Tumpey TM, Renshaw M, Clements JD, Katz JM. Mucosal delivery of inactivated influenza vaccine induces B-cell-dependent heterosubtypic cross-protection against lethal influenza A H5N1 virus infection. *J Virol* 2001;75(11):5141–50.
- [32] Griffiths CE, Dearman RJ, Cumberbatch M, Kimber I. Cytokines and Langerhans cell mobilisation in mouse and man. *Cytokine* 2005;32(2):67–70.
- [33] Treanor JJ, Campbell JD, Zangwill KM, Rowe T, Wolff M. Safety and immunogenicity of an inactivated subvirion influenza A (H5N1) vaccine. *N Engl J Med* 2006;354(13):1343–51.
- [34] Treanor JJ, Wilkinson BE, Maseoud F, Hu-Primmer J, Battaglia R, O'Brien D, et al. Safety and immunogenicity of a recombinant hemagglutinin vaccine for H5 influenza in humans. *Vaccine* 2001;19(13–14):1732–7.
- [35] Lin J, Zhang J, Dong X, Fang H, Chen J, Su N, et al. Safety and immunogenicity of an inactivated adjuvanted whole-virion influenza A (H5N1) vaccine: a phase I randomised controlled trial. *Lancet* 2006;368(9540):991–7.
- [36] Quan FS, Huang C, Compans RW, Kang SM. Virus-like particle vaccine induces protective immunity against homologous and heterologous strains of influenza virus. *J Virol* 2007;81(7):3514–24.